G-41-62

FINAL REPORT

STRUCTURAL LOCATION AND ROLE OF HYDROGEN IONS IN KAOLINITE AND ITS PRODUCTS IN ALUMINUM REMOVAL

By

R. A. Young
P. R. Suitch
W. E. Moody

Prepared for

BUREAU OF MINES
GRANTS MANAGEMENT BRANCH
WASHINGTON, D. C. 20241

Report Period covered 30 September 1981 to 29 September 1983

Under

Grant No. 1115131

December 1983

GEORGIA INSTITUTE OF TECHNOLOGY
A UNIT OF THE UNIVERSITY SYSTEM OF GEORGIA
SCHOOL OF PHYSICS AND
SCHOOL OF CERAMIC ENGINEERING
ATLANTA, GEORGIA 30332

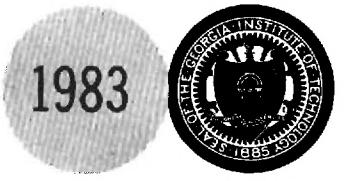

50272-101

REPORT DOCUMENTATION PAGE	1. REPORT NO.	2.	3. Recipient's Accession No.

4. Title and Subtitle
"Structural Location and Role of Hydrogen Ions in Kaolinite and its Products in Aluminum Removal"

5. Report Date
23 December 1983

6.

7. Author(s)
R. A. Young, P. R. Suitch and W. E. Moody

8. Performing Organization Rept. No.
G41-625-F

9. Performing Organization Name and Address
School of Physics and School of Ceramic Engineering
Georgia Institute of Technology, Atlanta, GA 30332

(404) 894-5208 (404) 894-2853

10. Project/Task/Work Unit No.

11. Contract(C) or Grant(G) No.
(C)
(G) 1115131

12. Sponsoring Organization Name and Address
Bureau of Mines
Grants Management Branch
Washington, D.C. 20241

13. Type of Report & Period Covered
FINAL-30 Sept. 1981 to 29 Sept. 1983

14.

15. Supplementary Notes

16. Abstract (Limit: 200 words)

A complete crystal structure refinement of kaolinite (specimens from Keokuk geodes) was achieved for the first time. Both x-ray and neutron powder diffraction data and the Rietveld method were used. The positions of the non-hydrogen atoms in dickite were similarly re-refined from x-ray powder data. In kaolinite, the rotation in the tetrahedral sheet is 7(1)°. The two inner hydroxyl O-H bonds are differently oriented; one points into an octahedral vacancy and the other somewhat away from the octahedral sheet. All six of the inner surface hydrogen atoms appear to be nearly equally involved in the hydrogen bonding between kaolinite layers in kaolinite.

The process of dehydroxylation of the kaolinite was followed in detail with x-ray diffraction techniques, including Rietveld analyses and infrared spectroscopy, in steps up to 465°C. Dehydroxylation began at about 325-350°C and was more than half completed at 465°C. It was found, however, that "half completed" means that half of the initial sample was completely dehydroxylated (and was presumably metakaolinite) while the other half was not at all dehydroxylated but retained all details of its kaolinite structure.

17. Document Analysis a. Descriptors

Kaolinite
Dickite
Crystal structure
Dehydroxylation
Atomic-scale features

b. Identifiers/Open-Ended Terms

c. COSATI Field/Group

18. Availability Statement	19. Security Class (This Report)	21. No. of Pages
	20. Security Class (This Page)	22. Price

(See ANSI-Z39.18) See Instructions on Reverse OPTIONAL FORM 272 (4-77)
(Formerly NTIS-35)
Department of Commerce

A. OBJECTIVES

The initially stated objectives were (1) to determine the mechanistic details by which the structural locations and ordering of the hydrogen ions in kaolinite affect its crystallinity, solubility, viscosity, processing, and use characteristics, (2) to determine the intra-crystalline mechanisms involved in the extraction of aluminum, and (3) to better determine and control the characteristics of the silicaceous by-products of aluminum extraction in order that useful products, such as zeolites, may be created from them.

B. APPROACH

Various naturally occuring clay characteristics and various regimens of heating, acid-leaching, deuteration, and irradiation were to be used as variables. Analytical studies were carried out primarily with x-ray and neutron powder diffraction analyses, especially the Rietveld whole-pattern-fitting-structure-refinement (PFSR) method, and with infrared spectroscopy used in a complementary mode. Any shifts in atom site-occupancies, positions and bonding were to be followed.

C. ACCOMPLISHMENTS

1. Crystal Structure of Kaolinite and Dickite

The refinement of the complete crystal structure of kaolinite represented a major effort. Most of the work came after we had shown that the Rietveld structure refinement method worked well with dickite and the initial refinements on kaolinite were successfully done. Much effort was devoted to multiple cross-checking of the results and to establishing and minimizing the probable errors. Two different samples and two different starting models, for each, were used in order to assess possible problems with false minima. The work done to accomplish these error assessments was detailed in the

Annual Progress Report for the period 30 September 1981 - 29 September 1982. That makes rather dull reading for most mineralogists, however, so much of it was omitted from our paper, describing the structural results, published in Clays and Clay Minerals, **31**, 357-366 (1983). A copy of the paper is included here as Appendix 1. Among the principal results are the following: (1) In kaolinite, the SiO_4 tetrahedra are rotated by 7(1)°, not 20° as had been reported (Zvyagin, 1960). This difference strongly affects Giese's electrostatic-energy-based calculations of the orientations of the inner-surface hydroxyls and they now agree with experiment (Giese and Datta, 1973; Giese, 1983). (2) All six of the inner-surface hydroxyls take part about equally in the hydrogen bonding between layers. (3) The unit cell is definitely triclinic; it is not indistinguishable from monoclinic as has recently been assumed (Adams, 1983). (4) The two inner hydroxyls are differently oriented. One points into an octahedral vacancy while the other points toward the unoccupied center of on oxygen triangle formed by the two apex oxygens and shared basal oxygen of two adjacent SiO_4 tetrahedra. (5) Except for the hydrogen atoms, the kaolinite layers in both kaolinite and dickite are very similar and are much as inferred (kaolinite) or determined (dickite) previously by others, notably G. W. Brindley and co-workers.

At the close of the work reported in the paper, there remained a possible question of two-fold disorder in the inner-surface hydroxyl z position. A possible displacement of $\pm$ 2 σ could not be ruled out. Greater precision would be required for this determination. The Intense Pulsed Neutron Source (IPNS) facility at Argonne National Laboratory appeared to have the potential for producing diffraction data which could lead to the required improvements in precision. We therefore made application for and were accepted as users of the IPNS, and collected IPNS diffraction data on Keokuk kaolinite at room temperature and at 10°K. Unfortunately, there is a

very high and non-linear background produced, from all of the hydrogen present, by incoherent scattering of thermal neutrons. We have determined that, for Rietveld structure analyses to go forward, it will be necessary to model explicitly the non-linear incoherent-scattering background in order to separate its effects from those of the non-linear energy spectrum in the Rietveld refinements.

An effort was undertaken to overcome the problem by deuterating a Keokuk kaolinite specimen in a hydrothermal bomb. That effort was aborted when, after about six weeks of continuous operation with this specimen, the hydrothermal bomb exploded (in a manner which the manufacturer had repeatedly assured us was impossible) and set fire to the laboratory in April 1983. Three months after the expiration of the project work period, the hydrothermal bomb unit has been replaced and special shielding is being built. We hope that we may, later, have the opportunity to prepare a specimen of deuterated Keokuk kaolinite and to collect diffraction data from it at the IPNS.

2. Dehydroxylation of Keokuk Kaolinite

2.1 Goals and Approach

It was desired to know in detail the atomic mechanism(s) by which kaolinite becomes dehydroxylated and transforms to metakaolinite upon being heated appropriately. One hope was that if progressive changes in atomic site occupancies or positions, or both, of the atoms could be followed, perhaps the understanding thereby developed could be used to tailor Aℓ removal procedures to improve the utilization of kaolinite as a source of aluminum. The strategy was to heat the same specimen repeatedly at successively higher temperatures and to do (at room temperature) quantitative i.r. (Perkin-Elmer 580B instrument operated in the absorbance mode) studies and x-

ray diffraction Rietveld structure refinements, of atom position and site occupancies as well as lattice parameters, after each heat. Since current computer programs for Rietveld analysis do not include nb/3 or other faulting in the model, it was necessary to use the very special, nearly faulting-free material, the Keokuk kaolinite. We were very fortunate to have enough, barely, of this material for the x-ray diffraction work.

2.2 Previous Work by Others

There is much controversy concerning the exact nature of partially dehydroxylated kaolinite. Structures for metakaolinite have been proposed by many authors who have drawn the following conclusions, not all of which are mutually tenable. (1) Upon the formation of metakaolinite, there is a c-axis lattice contraction while the a and b axes expand so as to allow the removal of the rotation of the individual tetrahedra in the tetrahedral sheet (Brindley and Gibbon (1968)). (2) Dehydroxylation causes a change in coordination number for Al^{+3} from six to four while Si^{+4} retains its coordination number of four and stabilizes the metakaolinite structure (Brindley and Nakahira (1959) and Freund (1967)). (3) The metakaolinite structure is either a 6-4-4 type oxygen atom distribution (Tscheischwili, Buessem, and Weyl (1939)) or a 6-6-2 type (Brindley and Nakahira (1959), and Pampuch (1966)). (4) The ex-kaolinite layers in metakaolinite retain their relic hexagonal crystal habit), as is shown by SEM photographs and only have two dimensional regularity in the a, b plane and complete disorder perpendicular to it , i.e., in the c direction (Brindley and Hunter (1955) and Roy, Roy and Francis (1955)). The structure of metadickite was determined to be a 6-4-4 type by Okada and Ossaka (1982) using radial distribution function analysis and x-ray data.

The mechanism of the transformation from kaolinite to metakaolinite has received the attention of several authors who produced conclusions not

inconsistent with each other. Toussiant, Fripiat, and Gastuche (1963) concluded that, as dehydroxylation occurs within the kaolinite structure, there is a random loss of "structural H_2O" and consequently the entire octahedral layer is destroyed. This mechanism was further clarified by Fripiat and Toussaint's (1963) conductometric measurements on kaolinite in the range 100 to 360°C. They noted that proton delocalization occurs with the free hybrid orbitals of oxygen in kaolinite, thus producing a precursor to "structural water" loss. Mitra and Bhattacherjee (1969) and Mitra and Bhattacherjee (1970) utilized x-ray diffraction line profile broadening studies to conclude that, as dehydroxylation proceeds with increasing temperature, the probability of layer shift (i.e. layer stacking disorder) and the variability of interlayer spacing increases. They proposed that these variations in kaolinite layer stacking were responsible for the loss of three dimensional periodicity in metakaolinite. One could expect that delocalization of the protons of the inner surface hydroxyls would, indeed, let the interlayer spacings increase as the hydrogen bonding was thereby weakened. Leonard (1977), utilizing radial electron density distribution and x-ray spectroscopy, confirmed this theory and added that, upon dehydroxylation, the kaolinite layers apparently do not collapse immediately into the more compact tetrahedral configuration of metakaolinite or the truncated octahedral configuration demonstrated by Iwai, Tagai and Shimamune (1971) in their single crystal investigation of partially dehydroxylated dickite at 535°C.

2.3 Results

The relative intensities of the x-ray diffraction peaks showed no obvious changes with heating temperature. Rietveld structure refinements, from x-ray powder diffraction data collected after each heat up to 455°,

showed no statistically significant changes in atomic positions nor site occupancies. The areas under the various i.r. absorption bands are shown as a function of heating temperature in Fig. 1 for specimen K34A and in Fig. 2 for K34B, the other half of the initial K34 specimen. (After the 455° heat, specimen K34A was lost to a runaway furnace.) Also shown plotted are (i) the maximum counts per 100 seconds in the strongest diffraction peak and (ii) the scale factor obtained in the Rietveld analysis performed after each heat. On the assumption of constant incident beam intensity, which is probably justified to better than 10%, both (i) and (ii) would be linearly related to the amount of crystalline kaolinite present. (A further assumption is that the peak breadth did not change. That assumption also, is essentially correct.)

It thus appears that, as dehydroxylation proceeded, some of the kaolinite was transformed but that the remainder was unchanged as "seen" by the x-rays and with i.r. spectroscopy. No precursor of metakaolinite was discernibly formed. No broadening of the peaks was observed. At the higher temperatures a rising background around 20°(2θ, with Cu Kα radiation) was observed (Fig. 3). It has not yet been determined whether this is an "amorphous hump" due to metakaolinite or a two-dimensional diffraction effect arising from the two-dimensionally ordered relic-kaolinite layers, or to both.

It should be noted that proton delocalization, per se, would not be detected in the x-ray structure refinements. The fact that all of the i.r. bands decrease in consort argues against large changes in hydrogen bonding prior to the break up of the whole crystal. A small amount would not have been detected here, so our results neither support nor contradict those of Toussiant and co-workers (1963).

Our conclusion is that, except for a possible small amount of precursor

proton delocalization, the transformation from kaolinite to metakaolinite does not proceed by stages in a given crystallite but goes all at once; a given crystallite either remains kaolinite or changes, probably precipitously, to metakaolinite with simultaneous re-arrangement of all atoms.

3.0 Further Information

Much further detail, data, and literature references about the kaolinite and dickite structures and about the dehydroxylation are given in a thesis now nearing completion by P.R. Suitch. He will submit it in partial fulfillment of the requirement for his M.S. in Chemistry, expected in March 1984.

4. References

1. Adams, J. M. (1983), "Hydrogen Atom Positions in Kaolinite by Neutron Profile Refinement," Clays and Clay Minerals, **31**, 352-356.

2. Brindley, G. W., and Gibbon, D. L. (1968), "Kaolinite Layer Structure: Relaxation by Dehydroxylation," Science, **162**, 1390-1391.

3. Brindley, G. W., and Hunter, K (1955), "The Thermal Rections of Nacrite and the Formation of Metakaolin, Y-Alumina, and Mullite," Min. Mag., **30**, 574-584.

4. Brindley, G. W. and Nakahira, M. (1959), "The Kaolinite-Mullite Reaction Series: II Metakaolin," J. Am. Cere. Soc., **42**, 314-318.

5. Freund, V. F. (1967) "Kaolinit - Metakaolinit, Model, Fall eines Festkorpers mit extrem hohen Storstellenkonzentrationen," Ber. DKG., **44**, 5-13.

6. Fripiat, J. J. and Toussaint, F. (1963), "Dehydroxylation of Kaolinite: II Conductiometric Measurements and Infrared Spectroscopy," J. Phys. Chem., **67**, 30-36.

7. Giese, R. F., Jr. (1982), "Theoretical Studies of the Kaolin Minerals: Electrostatic Calculations," Bull. Mineral., **105**, 417-424.

8. Giese, R. F., Jr., and Datta, P. (1973), "Hydroxyl Orientation in Kaolinite, Dickite, and Nacrite," Am. Mineral. **58**, 471-479.

9. Leonard, A. J. (1977), "Structural Analysis of the Transition Phases in the Kaolinite-Mullite Thermal Sequence," J. Am. Cere. Soc., **60**, 36-43.

10. Mitra, G. B., and Bhattacherjee, S. (1969), "X-ray Diffraction Studies on the Transformation of Kaolinite into Metakaolin: I. Variability of Interlayer Spacings," Am. Mineral., **54**, 1409-1418.

11. Mitra, G. B., and Bhattacherjee, S. (1970), "X-ray Diffraction Studies on the Transformation of Kaolinite into Metakaolin. II. Study of Layer Shift," Acta. Cryst., **B26**, 2124-2128.

12. Okada, K., and Ossaka, J. (1982), "Structural Analysis of Metadickite," J. Am. Cere. Soc., **65**, 21-24.

13. Roy, R., Roy, D. M., and Francis, E. E. (1955), "New Data on Thermal Decomposition of Kaolinite and Halloysite," J. Am. Cere. Soc., **38**, 198-205.

14. Toussaint, F., Frippiat, J. J., and Gaustuche, M. C. (1963), "Dehydroxylation of Kaolinite: I. Kinetics," J. Phys. Chem, **67**, 26-30.

15. Tscheischwili, L., Buessem,W., and Weyl, W., (1939) "Metakaolin," Ber. DKG., **20**, 249-276.

16. Zvyagin, B. B. (1960), "Electron Diffraction Determination of the Structure of Kaolinite," Kristallografiya, **5**, 32-41.

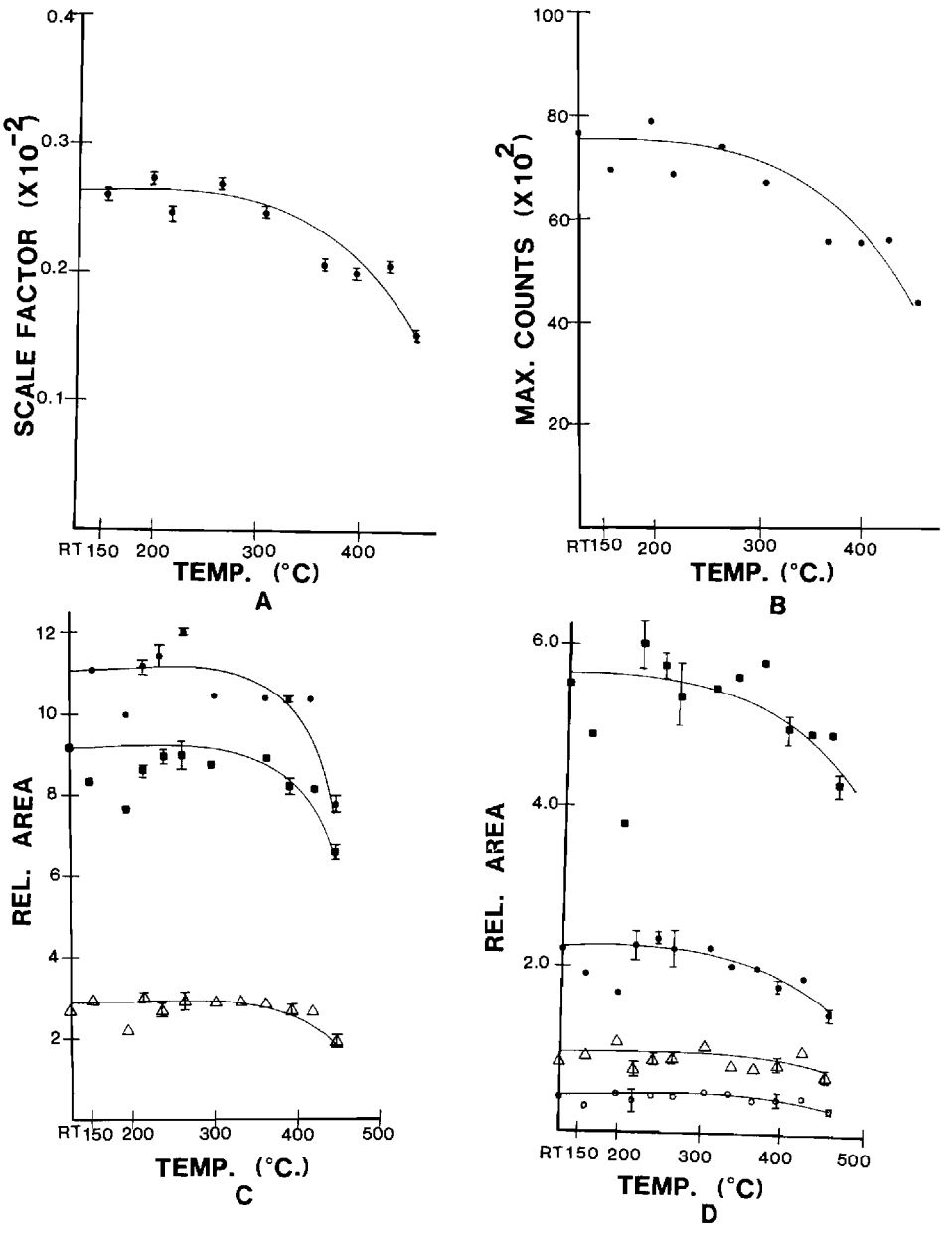

Figure 1: Results of the dehydroxylation studies on kaolinite (K-34A) from x-ray diffraction and IR. The scale factors obtained in the Rietveld analyses are shown in A and the number of counts per 100 seconds at the top of the 001 reflection are shown in B. The circles, squares and triangles in C represent the effect of dehydroxylation on the relative peak areas for the Al-O-Si, Al-OH and Si-O vibrations, respectively. The squares, circles, triangles and open circles in D represent the effect of dehydroxylation on the OH vibrations at 3697, 3624, 3656 and 3672 cm^{-1}, respectively.

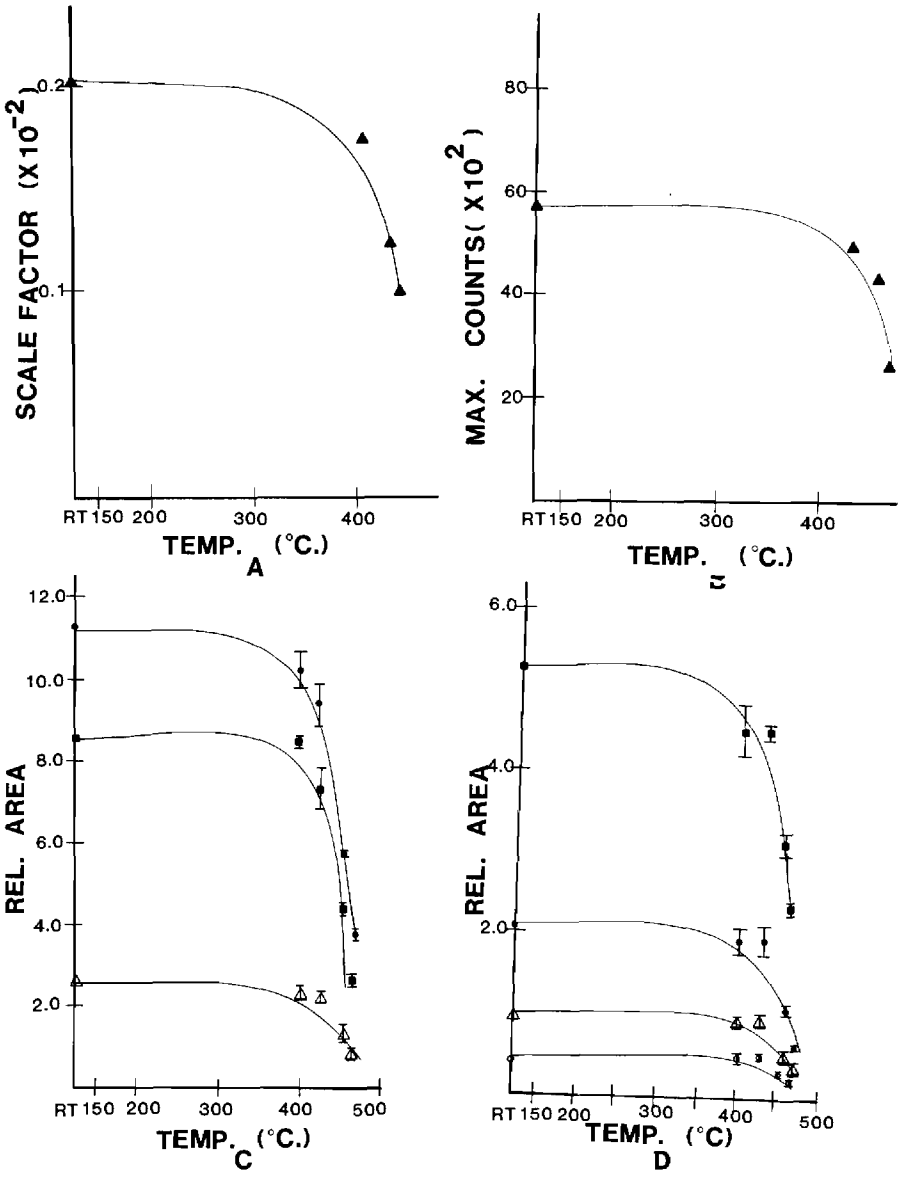

Figure 2: Results of the dehydroxylation studies on kaolinite (K-34B) from x-ray diffraction and IR. Format is as for figure 1.

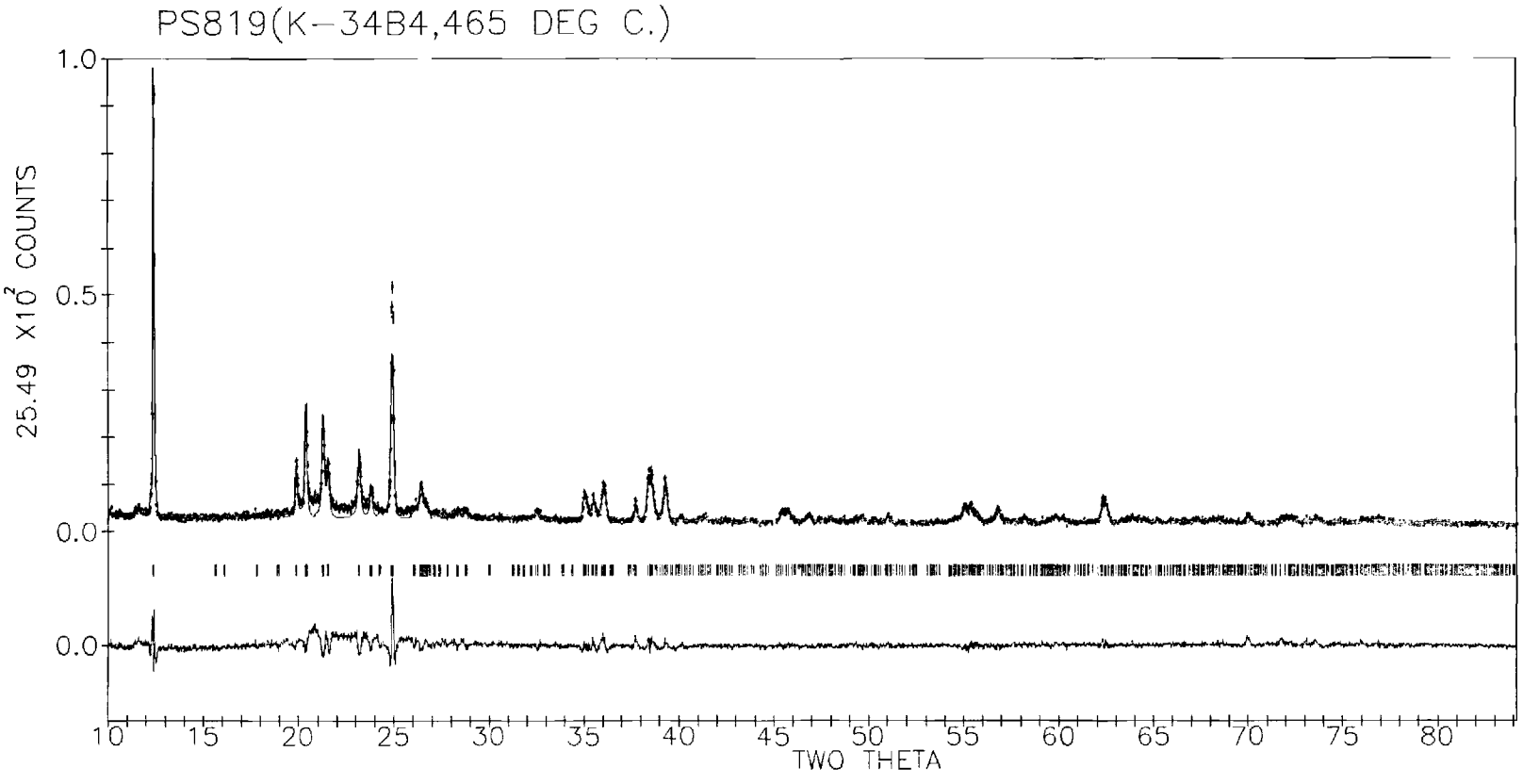

Figure 3: X-ray pattern-fitting plot, for a kaolinite sample that was heated for 24 hours at 455°C, showing result of the Rietveld refinement of its structure from the Suitch and Young (1983) model. In the upper field in each plot, the observed data are shown as dots with vertical error bars through them and the calculated pattern is shown as a solid curve. The difference (observed minus calculated) is shown in the lower field. The short vertical bars in the middle field mark the positions of possible Bragg reflections. The large "hump" that occurs between 16° and 26°(2θ), best seen ion the difference plot, is due to the formation of metakaolinite, or to nb/3 shifting of the kaolinite layers, or to both.

APPENDIX I

Reprint of published paper on "Atom Positions in Highly Ordered Kaolinite".

Note: The following errata occur in the publication:

"The footnote to Table 2 should read "BRR is the result of our Rietveld structure refinements started from the Brindley and Robinson (1946) model. ZR is the result of our refinements started from the Zvyagin (1960) model and ZRT is that result transformed to the BRR cell setting. NRT is the result of refinement started from the Newnham (1961) model of dickite and then transformed to the BRR kaolinite cell. In the caption of Fig. 3, BR should be BRR."

Clays and Clay Minerals, Vol. 31, No. 5, 357–366, 1983.

ATOM POSITIONS IN HIGHLY ORDERED KAOLINITE

P. R. SUITCH AND R. A. YOUNG

School of Physics, Georgia Institute of Technology, Atlanta, Georgia 30332

Abstract—The crystal structure of kaolinite ($P1$, $a = 5.153$ (1), $b = 8.941$ (1), $c = 7.403$ (1) Å, $\alpha = 91.692(3)°$, $\beta = 104.860(3)°$, $\gamma = 89.822(3)°$, specimens from Keokuk geodes) has been refined in detail and that of dickite (Cc, $a = 5.1460(3)$, $b = 8.9376(5)$, $c = 14.4244(6)$ Å, $\beta = 96.761(5)°$) has been re-refined, both from powder diffraction data with the Rietveld method. Except for the hydrogen atoms, the layer structures in both clays are very similar and are much as inferred or determined previously by others. The rotation in the tetrahedral sheet is 7(1)°. The two inner hydroxyl O–H bonds in kaolinite are differently oriented; one points into an octahedral vacancy and the other somewhat away from the octahedral sheet and toward the unoccupied center of an oxygen triangle formed by the two apical oxygens and shared basal oxygen of two adjacent SiO_4 tetrahedra. All six of the inner surface hydrogen atoms appear to be nearly equally involved in the hydrogen bonding between kaolinite layers in kaolinite.

Key Words—Crystal structure, Dickite, Hydrogen atom, Hydroxyl orientation, Kaolinite, Rietveld method.

INTRODUCTION

Kaolinite, dickite, and nacrite are based on essentially the same structural element, a layer of composition $Al_2Si_2O_5(OH)_4$. Each of these basic layers can be regarded as consisting of a tetrahedral sheet of SiO_4 tetrahedra and an octahedral sheet of Al octahedrally coordinated by O and OH. Alternatively, one may think of the layer as being composed of five planes of atoms stacked together and consisting of, successively, O, Si, (O, OH), Al, and OH (e.g., Norton, 1973). The actual positions of the non-hydrogen atoms in kaolinite were deduced rather closely by Brindley and Robinson (1946), who also determined that the actual crystal lattice was triclinic with probable space group $P1$. Later, Brindley and Nakahira (1958) deduced that some distortions exist in the octahedral sheet and that the SiO_4 tetrahedra are rotated about 10° from their earlier assigned symmetric positions. From an electron diffraction structure study (excluding H atoms), Zvyagin (1960) inferred that the silicate tetrahedra are rotated about 20° from Brindley and Robinson's symmetrical positions. Positions thought to be probable for the H atoms were reported by Giese and Datta (1973) on the basis of energy calculations, previous infrared studies, and the Zvyagin (1960) model.

The structure of dickite, except for the hydrogen atoms, was refined by Newnham and Brindley (1956, 1957) and was further refined by Newnham (1961) from single-crystal X-ray diffraction data. Newnham's 1956 results were used by Brindley and Nakahira (1958) to improve the structural model of the kaolinite layer. The similarity of dickite and kaolinite has been further emphasized by Bailey (1963) who demonstrated that an equally valid and mineralogically preferred choice of unit cell for dickite leads to $\beta = 103.58°$, almost identical to that for kaolinite, rather than the $\beta = 96.73°$ value arising from Newnham's (1961) choice of cell. Kaolinite and dickite, however, do have some marked differences: (1) no kaolinite single crystals of size usable for X-ray diffraction structure studies are known; (2) layer stacking disorder (nb/3 shifts) is all but ubiquitous in kaolinite from all sources, whereas dickite rarely exhibits such disorder (Brindley and Porter, 1978); and (3) thirteen non-H atoms are present in the asymmetric unit of dickite, and four of these units combine according to space group Cc to make up the unit cell. The asymmetric unit of kaolinite (which is the entire unit cell, space group $P1$) contains 26 non-H atoms in two pseudo-equivalent sets of 13, each similar to the 13 non-H atoms in dickite. Considering the near identity of the "kaolinite layer" in dickite to that in kaolinite, the questions arise as to just how nearly identical are they in detail and how can the differences in crystallization and disorder be explained? The present work presents a detailed structure refinement of kaolinite and a re-refinement of the structure of dickite using the Rietveld method to answer these questions.

MATERIALS AND METHODS

Kaolinite from geodes found near Keokuk, Iowa, was kindly provided by Dr. W. D. Keller. Kaolinite from this general locality (Hayes, 1963; Keller *et al.*, 1966) is remarkable in that much of it is essentially free of the nb/3 shifting that is characteristic of kaolinite from other sources. The lack of nb/3 shifting was crucial to the success of this study because including its effects in the structure refinement would be a non-trivial task and has not been done. Two samples showing the least nb/3 shifting were selected, and the <37-μm particle size fractions were used as the study specimens (K27A and K31A).

Dickite from Ouray, Colorado, obtained from Wards

Natural Science Establishment, Rochester, New York (H-14), was also examined.

X-ray powder diffraction data were collected with crystal-monochromated CuKα radiation (λ = 1.5405 and 1.5443 Å) and a diffractometer operating in the step-scan mode at 100 sec/0.0375°2θ step (0.05° for dickite) over the 2θ range 10°–104°. Neutron powder diffraction data were collected from specimen K31A at Brookhaven National Laboratory by the courtesy and with the assistance of D. E. Cox. Because of the large incoherent scattering of thermal neutrons by hydrogen, a "third axis" was used to eliminate most of the inelastic portion of it. Most of the incoherent scattering is elastic, however, and it so degraded the signal-to-noise ratio that two full days of operation were required to produce a usable pattern over the 2θ range 17°–126° with λ = 2.3850 Å.

The structure refinements were carried out from both X-ray and neutron powder diffraction data with the Rietveld method (Rietveld, 1969; Young and Wiles, 1981). Version DBW 3.2 of a locally written computer program (Wiles and Young, 1981) was used with a pseudo-Voigt profile function.

Lattice parameters were refined simultaneously with the atomic parameters and other needed parameters (e.g., zero point, reflection profile breadth, background, asymmetry, preferred orientation) and an overall temperature factor. Test refinements with individual isotropic temperature factors, fixed in both kaolinite and dickite at the values given by Newnham (1961) showed that the positional parameters were not affected by using only an overall temperature factor instead of the fixed individual isotropic temperature factors. For most of the refinements with X-ray data, only the range $10° \leq 2\theta \leq 81°$ was used because (1) the very large number of Bragg reflections tended to produce some computational difficulties, and (2) the severe multiple overlapping of reflections in the higher region tended to diminish the amount of extractable information. Test refinements with the atom site occupancies that were varied simultaneously with the other parameters did not indicate any significant departure from stoichiometry. The site occupancies were henceforth fixed at unity; however, the data used in these refinements do not extend effectively over a $(\sin\theta)/\lambda$ range large enough to support simultaneous refinement of thermal factors and site occupancies nor to provide precision better than ~10% when only site occupancies were refined with the thermal parameters kept fixed.

The dickite structure (except for H atoms) was refined from X-ray powder diffraction data primarily to assure that the refinement procedures were working properly, as judged by the agreement of our results with pre-existing single crystal results of Newnham (1961).

The non-H portion of the kaolinite structure was then refined for both specimens K27A and K31A: (1) starting from the Brindley and Robinson (1946) coordinates (BRO model), and (2) starting from Zvyagin's (1960) coordinates (ZO model). In each refinement, the starting positions for the second set of 13 atoms were generated by application of ½a + ½b to the coordinates given by the cited authors for the first set of 13. Because the actual kaolinite atom positions in space group $P\bar{1}$ are close to those demanded for C-face centering, this procedure produced usable starting parameters for all 26 non-H atoms. The purposes in working with the two starting models were to test each directly for correctness and to assure that the same refined model would result from different starting parameters, i.e., that there were no false minima in the neighborhood. The refinements made with the X-ray data included tests for O(H) disorder about the average plane of the OH sheet (no positive result). The H and associated O(H) positions were then refined from the neutron data (K31A only). For the refinements with neutron data, all atoms other than H and O(H) were fixed at the positions determined from the X-ray data. Again, two different starting models were used: (1) model GDO was based on the H positions postulated by Giese and Datta (1973), and (2) model AHO was based on the H positions determined in dickite by Adams and Hewat (1981) from Rietveld refinements with neutron powder diffraction data. As with the X-ray refinements, the atom positions in the second half cell of the starting models were generated from those in the first half by C-face centering.

The principal criteria for the success of the Rietveld refinements were R values, the appearance of pattern-fitting plots (e.g., Figure 1) and, as in any crystal structure refinement, stereochemical reasonableness of the refined structure. The two types of R values most considered were R_{wp} ("R weighted pattern") and R_B ("R Bragg"), as follows:

$$R_{wp} = \left[\sum_i w_i(y_i(o) - y_i(c))^2 / \sum_i w_i(y_i(o))^2 \right]^{1/2} \quad \text{and} \qquad (1)$$

$$R_B = \sum_H |I_H(\text{"o"}) - I_H(c)| / \sum_H I_H(\text{"o"}), \qquad (2)$$

where y_i is the intensity at the i^{th} step in the pattern, o and c indicate observed and calculated, respectively, w_i is the weight, H signifies the Miller indices *h, k,* and *l*, I_H is the intensity of Bragg reflection H, and "o" means that the intensity I("o") was not observed independently for overlapped reflections but was the portion of the total overlapped intensities allocated to the H^{th} reflection on the basis of calculated intensity ratios. A discussion of the role of each of these fitting criteria has been given by Young and Wiles (1981).

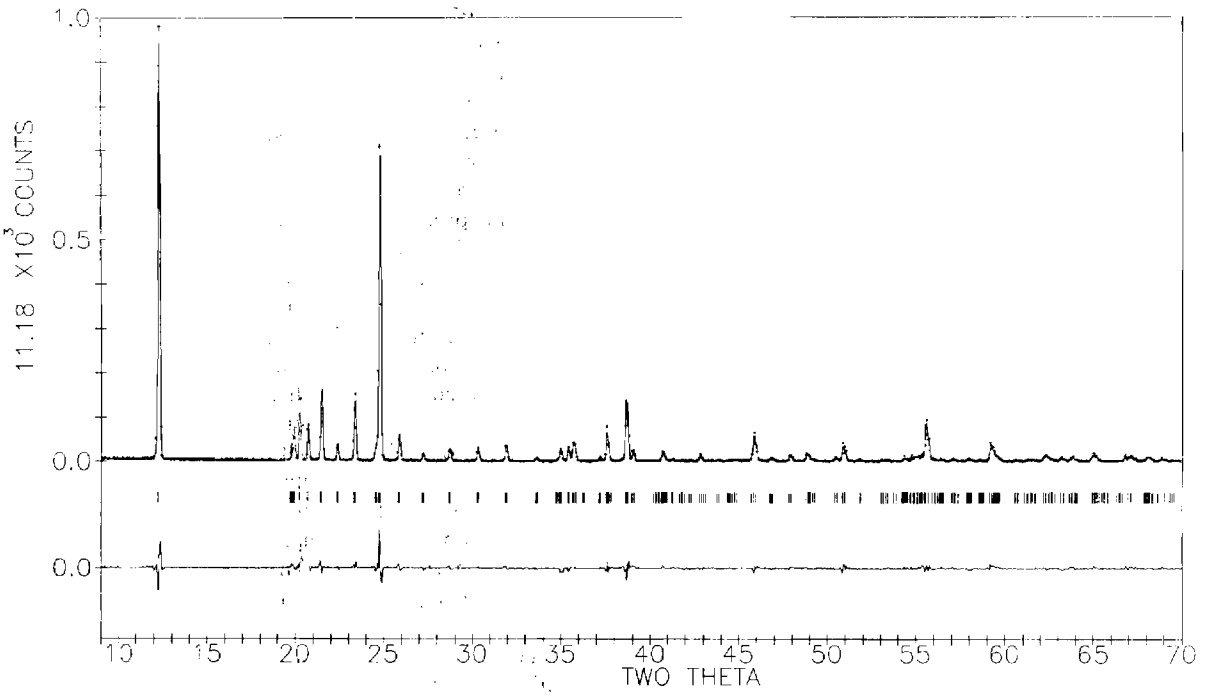

Figure 1. Pattern-fitting plot for Rietveld refinement of the dickite structure with X-ray diffraction data. In the upper field, the observed data are shown as dots with vertical error bars through them, and the calculated pattern is shown as the solid curve. The difference (observed minus calculated) is shown in the lower field. The short vertical bars in the middle field mark the positions of possible Bragg reflections.

RESULTS

Test of procedure with dickite

The results for the refinements of the dickite structure from X-ray powder diffraction data are shown in Table 1 and Figure 1. Using Newnham's (1961) estimated precision of 0.02 Å as the standard deviation, only 2 structural parameters (y of OH(1) and x of O(H7) differ by as much as 4 σ (combined) between his results and ours and 3 which differ by about 3 σ (z of O(6), x of O(9), and y of Si(3)). Thus, the present Rietveld structure refinement results based on powder data are in good agreement with Newnham's single crystal results within the limits to be expected on the basis of the combined estimated standard deviations obtained from those calculated in the Rietveld procedure procedure and those estimated by Newnham (1961). It was therefore concluded that the Rietveld structure refinement procedure was appropriate for this problem.

Kaolinite structural results and tests for model and specimen dependence

With two exceptions, lattice parameters and a possible pattern in O(H) z parameter differences, the X-ray structural results obtained for the two kaolinites using the two starting models (BRO and ZO) did not differ significantly. Therefore, only the results for K31A are presented in Table 2 and Figure 2. The lattice parameters obtained for K27A were $a = 5.1543(2)$, $b = 8.9423(4)$, $c = 7.4032(3)$ Å, and $\alpha = 91.706(3)$, $\beta = 104.859(3)$, $\gamma = 89.818(3)°$. These values differ at most by $\sim 3\,\sigma$(combined) from those of sample K31A (Table 2). The e.s.d.'s on the structural parameters were generally 10–20% larger for sample K27A than for sample K31A. It may be relevant that only a small amount of nb/3 shift was discernable in the X-ray powder diffraction pattern of sample K27A. No shifting was detectable in the pattern of sample K31A (Figure 2).

To compare ZR and BRR, and thus to see if both starting models had led to the same result, it was necessary to determine the optimum transformation between the cells. (Because the space group is $P1$, the selection of the cell origin is completely arbitrary.) Normal projections of the two structures, BRR and ZR, onto the a,b plane were plotted as shown in Figure 3. Transparencies of these plots were then rotated and translated as necessary to produce the best visual fit of the two structures. This procedure produced the empirical transformation rule:

$$x_{BRR} = \bar{x}_{ZR} + 0.323;$$
$$y_{BRR} = \bar{y}_{ZR} + 0.148;$$
$$z_{BRR} = \bar{z}_{ZR} + 0.449. \quad (3)$$

This transformation was applied to the ZR results which

Table 1. Crystal structural parameters for dickite.

	Atomic coordinates					
	This work			Newnham (1961)		
	x	y	z	x	y	z
Al(2)	0.407(9)	0.425(2)	0.238(2)	0.419	0.417	0.231
Al(3)	0.921(7)	0.257(2)	0.238(2)	0.915	0.253	0.232
Si(2)	0.477(7)	0.572(2)	0.043(2)	0.500	0.573	0.040
Si(3)	−0.015(8)	0.405(2)	0.044(2)	0.012	0.400	0.041
O(2)	0.484(7)	0.585(4)	0.156(2)	0.511	0.581	0.153
O(5)	0.234(9)	0.475(4)	0.002(3)	0.259	0.472	−0.006
O(6)	0.066(12)	0.380(3)	0.164(3)	0.080	0.388	0.152
O(8)	−0.051(8)	0.238(5)	0.001(2)	−0.045	0.237	−0.006
O(9)	0.731(9)	0.501(3)	0.013(3)	0.765	0.511	0.006
O(H1)	0.589(9)	0.301(4)	0.168(3)	0.582	0.276	0.157
O(H4)	0.746(12)	0.391(4)	0.308(3)	0.747	0.395	0.298
O(H6)	0.333	0.587(5)	0.296	0.333	0.583	0.296
O(H7)	0.203(9)	0.267(5)	0.304(2)	0.244	0.273	0.295

	Other data					
	a (Å)	b (Å)	c (Å)	β (deg)	R_{wp} (%)	R_B (%)
This work	5.1460(3)	8.9376(5)	14.4244(6)	96.761(5)	18.05	4.37
Newnham	5.150(1)	8.940(1)	14.424(2)	96.73(2)		

Table 2. Positional parameters from X-ray diffraction data for kaolinite (BRR and ZRT) and for dickite expressed in the kaolinite cell (NRT).[1]

	BRR			ZRT			NRT		
Atom	x	y	z	x	y	z	x	y	z
Al(1)	0.367(12)	0.490(6)	0.443(7)	0.353(10)	0.500(6)	0.434(7)	0.335(7)	0.480(2)	0.443(2)
Al(2)	0.339(13)	0.824(6)	0.425(7)	0.352(11)	0.815(6)	0.449(7)	0.349(9)	0.812(2)	0.443(2)
Al(3)	0.846(15)	−0.006(8)	0.442(9)	0.862(11)	−0.016(6)	0.449(7)	0.835(7)	−0.020(2)	0.443(2)
Al(4)	0.847(14)	0.314(7)	0.457(7)	0.834(11)	0.322(6)	0.431(7)	0.849(9)	0.312(2)	0.443(2)
Si(1)	0.047(12)	0.322(6)	0.070(7)	0.043(10)	0.309(6)	0.045(7)	0.066(8)	0.332(2)	0.055(2)
Si(2)	0.061(12)	0.662(6)	0.054(7)	0.073(10)	0.656(7)	0.059(10)	0.071(7)	0.665(2)	0.053(2)
Si(3)	0.544(14)	0.831(7)	0.048(7)	0.546(11)	0.822(6)	0.070(6)	0.566(8)	0.832(2)	0.055(2)
Si(4)	0.579(14)	0.156(7)	0.064(8)	0.569(12)	0.161(5)	0.057(7)	0.571(7)	0.165(2)	0.053(2)
O(1)	0.110	0.342	0.307	0.105(14)	0.340(9)	0.290(10)	0.114(12)	0.357(3)	0.295(3)
O(2)	0.170(17)	0.652(8)	0.278(10)	0.169(13)	0.667(7)	0.286(8)	0.181(7)	0.652(4)	0.279(2)
O(3)	0.039(15)	0.474(8)	−0.028(8)	0.067(16)	0.505(9)	−0.030(13)	0.053(8)	0.499(5)	−0.031(2)
O(4)	0.267(16)	0.228(7)	−0.011(8)	0.261(17)	0.212(8)	−0.004(9)	0.281(9)	0.236(3)	−0.007(3)
O(5)	0.252(16)	0.754(9)	−0.034(10)	0.244(16)	0.761(7)	−0.021(10)	0.270(9)	0.762(4)	−0.029(3)
O(6)	0.612(22)	0.836(11)	0.295(12)	0.616(14)	0.836(8)	0.294(9)	0.614(12)	0.857(3)	0.295(3)
O(7)	0.679(13)	0.167(8)	0.279(9)	0.677(15)	0.152(7)	0.279(8)	0.681(7)	0.152(4)	0.279(2)
O(8)	0.563(15)	0.004(8)	−0.026(9)	0.532	−0.029	−0.026	0.553(8)	−0.001(5)	−0.031(2)
O(9)	0.749(16)	0.714(7)	0.000(9)	0.758(17)	0.727(7)	−0.005(8)	0.781(9)	0.736(3)	−0.007(3)
O(10)	0.751(16)	0.263(8)	−0.020(9)	0.754(17)	0.253(8)	−0.036(9)	0.770(9)	0.262(4)	−0.029(3)
O(H1)	0.127(16)	−0.039(8)	0.307(9)	0.100(14)	−0.031(7)	0.273(9)	0.079(9)	−0.064(4)	0.303(3)
O(H2)	0.022(16)	0.158(9)	0.582(9)	0.012(16)	0.162(8)	0.554(8)	−0.009	0.150(5)	0.569
O(H3)	0.095(18)	0.462(9)	0.585(9)	0.108(12)	0.465(8)	0.571(9)	0.124(9)	0.470(5)	0.575(2)
O(H4)	0.101(14)	0.841(8)	0.590(8)	0.094(14)	0.851(6)	0.553(7)	0.071(12)	0.846(4)	0.583(3)
O(H5)	0.608(13)	0.468(8)	0.270(8)	0.640(12)	0.460(7)	0.303(9)	0.579(9)	0.436(4)	0.303(3)
O(H6)	0.513(17)	0.664(9)	0.558(9)	0.523(13)	0.660(8)	0.582(8)	0.491	0.650(5)	0.569
O(H7)	0.597(13)	−0.033(8)	0.570(8)	0.581(14)	−0.036(7)	0.583(10)	0.624(9)	−0.030(5)	0.575(2)
O(H8)	0.577(16)	0.351(9)	0.557(9)	0.586(15)	0.340(8)	0.590(9)	0.571(12)	0.346(4)	0.583(3)

	Other results from X-ray data								
	a (Å)	b (Å)	c (Å)	α (deg)	β (deg)	γ (deg)	R_{wp} (%)	R_B (%)	R_{exp} (%)
BRR	5.1534(2)	8.9409(4)	7.4028(3)	91.692(3)	104.860(3)	89.821(3)	14.03	3.01	6.00
ZRT	5.1534(2)	8.9409(4)	7.4028(3)	91.692(3)	104.860(3)	89.822(3)	14.05	2.92	6.00

[1] BRR = Brindley and Robinson (1946); ZRT = Zvyagin (1960); NRT = Newnham (1961).

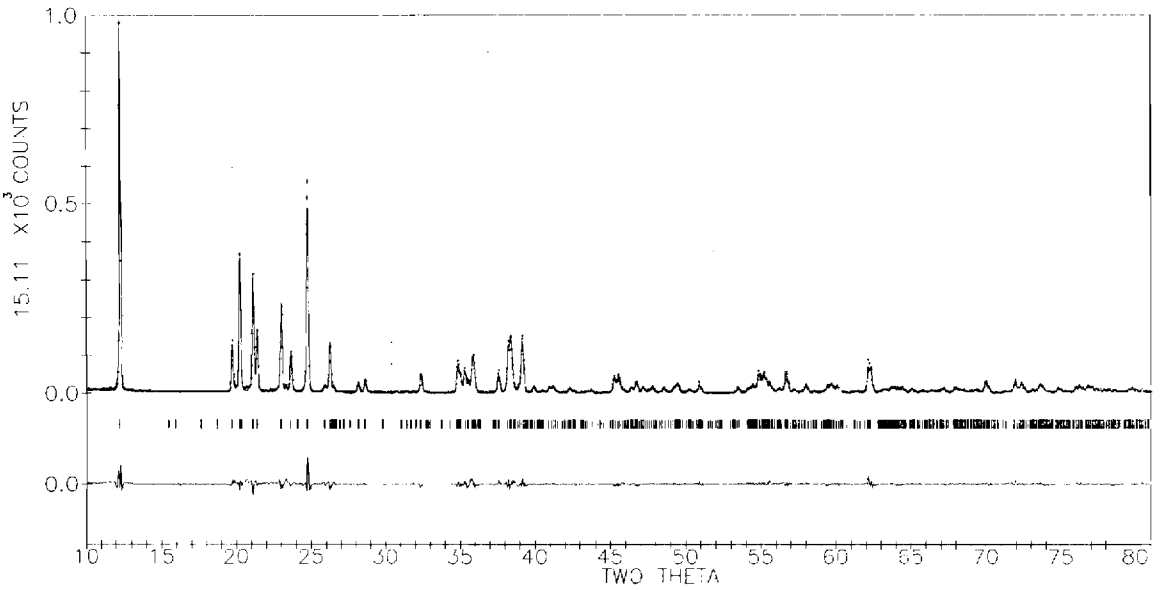

Figure 2. Pattern-fitting plot for Rietveld refinement of the structure of Keokuk kaolinite specimen K-31A with X-ray diffraction data, started from the Brindley and Robinson model (BRO) (see text). The format is as for Figure 1.

were obtained with the use of ZO as the starting model; the transformed results for sample K31A are given in Table 2 as ZRT. If the standard deviations in the individual parameters are considered, the ZR and BRR results are not significantly different. Only 2 of the 78 parameters differ by $>3\,\sigma$ and 9 others by $>2\,\sigma$, much as could be expected for a normal distribution of errors. From such an atom by atom consideration it was concluded that the same refined structure was obtained no matter which set of starting parameters was used.

Further examination of the BRR results in Table 2 shows that, within the precision reported here, the non-H atom portions in kaolinite are consistent with the space group $C1$. However, the positions found for the inner hydroxyl H and the lattice parameters (especially the α angle) confirm that the space group is, instead, $P1$.

Test for two-fold disorder in the O(H) sheet

Starting-model-dependent differences in the z coordinates of the inner surface hydroxyls are not readily apparent in individual groups of atoms. In both models, hydroxyl oxygen atoms (H 2, 3, 4, 6, 7, 8) were placed almost exactly on a plane, i.e., all 6 had almost the same z coordinates in each model. It can be seen from Table 2 that the O(H) atoms in the first half cell (H 2, 3, and 4) refined to positions "above" (larger z) the starting plane, and those in the second half cell, to nominal positions below the starting plane for starting model BRO. For starting model ZO, just the opposite configuration is apparent (see ZRT in Table 2). The same result was obtained with sample K27A. These observations may be thought to suggest that the inner surface O(H) atoms are actually in two-fold disorder about the average plane, as though their potential wells have double minima in z. Inasmuch as the separation of these hypothetical minima is only of the order of 2 or 3 σ, such disorder cannot be confirmed with the present data. Further, the neutron-based AHR and GDR refinements do not show this same pattern.

Rotation of SiO_4 tetrahedra

The largest differences between the starting and final, refined models for the non-H atoms in kaolinite can be described as rotations of the SiO_4 tetrahedra. These "rotations in the tetrahedral sheet" are primarily about

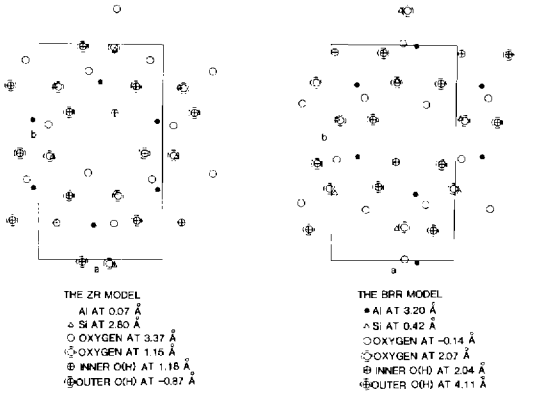

Figure 3. Comparison of the structure refined from the Brindley and Robinson model (BR) with that refined from the Zvyagin model (ZR). The projection is perpendicular to the a,b plane, and the numerical data are distances from it.

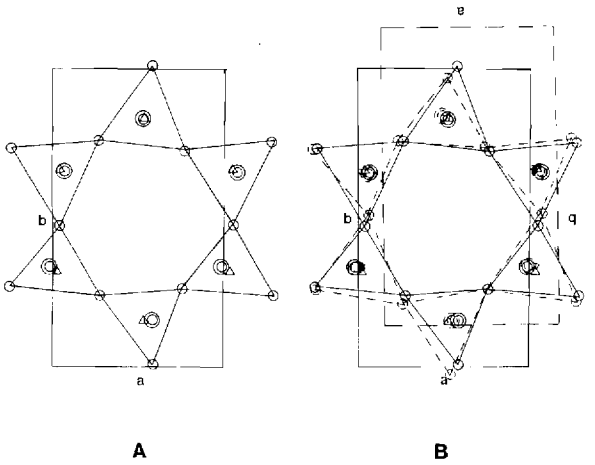

Figure 4. The tetrahedral sheets in the refined kaolinite structures projected onto the a,b plane. (a) In the BRR model, △ is Si, ◎ is oxygen, and O is oxygen at 2.70, 1.09, and 3.23 Å, respectively, from the plane. (b) Superposition of the tetrahedral sheets in the BRR model (solid lines) and the ZR model (dashed lines) in visually judged best-fit positions. Note that, although the cell settings are different, the two models do describe the same final structure.

an axis perpendicular to the a,b plane, to which plane one face of each SiO_4 tetrahedron is essentially parallel. (It is the oxygens on these faces that comprise the oxygen plane.) As a first approximation, Brindley and Robinson (1946) placed the tetrahedra rather symmetrically. Brindley and Nakahira (1958) suggested that a rotation of about 10° was probable. Zvyagin (1960) postulated a much larger rotation of 20°. The result with sample K31A is shown in Figure 4. The various tetrahedra are not obviously symmetric nor identically rotated. These imperfections, however, are mostly a matter of scatter of the representative atom-location points within a 3 σ range. From measurements of the angles between O face-edge lines in Figure 4 and from similar measurements for sample K27A, the average rotation of the tetrahedra is 7(1)°, substantially less than the value inferred by Zvyagin, but close to that inferred by Brindley and Nakahira (10°) and the same as that reported (8°) for dickite by Newnham and Brindley (1956). The importance of these rotations is attested to by Giese's (R. F. Giese, Jr., State University of New York at Buffalo, Amherst, New York, private communication, 1982) new energy-minimization cal-

Table 3. The O(H) and H positions in kaolinite (K-31A), Keokuk, Iowa.

	Refinement result AHR			Refinement result GDR		
	x	*y*	*z*	*x*	*y*	*z*
O(H1)	0.149(10)	0.191(6)	0.132(7)	0.199(12)	0.173(6)	0.131(7)
O(H2)	0.329(10)	−0.002(6)	−0.100(7)	0.327(14)	−0.007(6)	−0.110(8)
O(H3)	0.205(11)	0.691(6)	−0.133(9)	0.226(12)	0.677(6)	−0.125(8)
O(H4)	0.225(13)	0.296(6)	−0.124(8)	0.223(12)	0.301(6)	−0.112(7)
O(H5)	0.736(11)	0.679(5)	0.153(8)	0.669(10)	0.708(5)	0.146(8)
O(H6)	0.797(10)	0.502(6)	−0.133(8)	0.820(13)	0.507(6)	−0.105(8)
O(H7)	0.735(11)	0.171(6)	−0.114(8)	0.704(11)	0.186(6)	−0.113(8)
O(H8)	0.723(14)	0.814(7)	−0.133(9)	0.721(13)	0.806(6)	−0.145(8)
H(1)	0.070(17)	0.110(8)	0.087(10)	0.083(14)	0.106(7)	0.068(11)
H(2)	0.125(14)	−0.050(7)	−0.271(11)	0.168(13)	0.016(8)	−0.257(11)
H(3)	0.240(15)	0.640(10)	−0.235(12)	0.207(16)	0.636(9)	−0.279(1)
H(4)	0.255(15)	0.339(8)	−0.257(12)	0.278(14)	0.344(9)	−0.236(11)
H(5)	0.600(17)	0.585(8)	0.180(12)	0.617(16)	0.574(8)	0.179(11)
H(6)	0.712(15)	0.533(9)	−0.240(12)	0.520(12)	0.432(7)	−0.270(9)
H(7)	0.712(15)	0.142(9)	−0.285(11)	0.753(16)	0.149(10)	−0.254(13)
H(8)	0.745(19)	0.862(10)	−0.222(12)	0.728(14)	0.870(9)	−0.256(13)
	Starting model AHO			Starting model GDO		
	x	*y*	*z*	*x*	*y*	*z*
H(1)	0.127	0.083	0.207	0.133	0.094	0.120
H(2)	0.150	−0.008	−0.255	0.227	0.012	−0.271
H(3)	0.193	0.629	−0.263	0.273	0.669	−0.262
H(4)	0.209	0.356	−0.285	0.353	0.414	−0.159
H(5)	0.627	0.583	0.207	0.633	0.594	0.120
H(6)	0.650	0.492	−0.255	0.727	0.512	−0.271
H(7)	0.693	0.129	−0.263	0.773	0.169	−0.262
H(8)	0.709	0.856	−0.285	0.853	0.914	−0.159

R values

Refinement				
No.	Result	R_{wp} (%)	R_{exp} (%)	R_B (%)
RK171	AHR	5.50	5.26	1.02
RK173	GDR	5.51	5.26	1.08

Table 4. Interatomic distances (Å) and angles (°) for kaolinite.

O–O distances	
O(1)–O(2)	2.95(10)
O(1)–O(3)	2.79(11)
O(1)–O(4)	2.73(11)
O(1)–O(7)	2.76(11)
O(1)–O(10)	2.71(9)
O(2)–O(3)	2.85(10)
O(2)–O(5)	2.79(10)
O(2)–O(6)	2.50(10)
O(2)–O(9)	2.71(10)
O(3)–O(4)	2.65(9)
O(3)–O(5)	2.79(11)
O(3)–O(6)	2.59(10)
O(3)–O(9)	2.46(10)
O(3)–O(10)	2.56(11)
O(4)–O(1)	2.77(11)
O(4)–O(3)	2.73(11)
O(4)–O(7)	2.80(11)
O(4)–O(8)	2.65(9)
O(4)–O(10)	2.59(8)
O(5)–O(6)	2.59(12)
O(5)–O(8)	2.76(9)
O(5)–O(9)	2.40(7)
O(6)–O(7)	2.54(12)
O(6)–O(8)	2.87(10)
O(6)–O(9)	2.72(7)
O(7)–O(8)	2.80(10)
O(7)–O(10)	2.68(6)
O(8)–O(9)	2.65(10)
O(8)–O(10)	2.46(7)

Si–O distances	
Si(1)–O(1)	1.76(9)
Si(1)–O(3)	1.70(10)
Si(1)–O(4)	1.63(10)
Si(1)–O(10)	1.60(9)
Si(2)–O(2)	1.56(8)
Si(2)–O(3)	1.48(10)
Si(2)–O(5)	1.52(10)
Si(2)–O(9)	1.70(10)
Si(3)–O(5)	1.62(9)
Si(3)–O(6)	1.71(8)
Si(3)–O(8)	1.52(5)
Si(3)–O(9)	1.61(10)
Si(4)–O(4)	1.60(10)
Si(4)–O(7)	1.60(8)
Si(4)–O(8)	1.78(5)
Si(4)–O(10)	1.56(10)

O–Si–O angles	
O(1)–Si(1)–O(4)	107(4)
O(1)–Si(1)–O(10)	108(5)
O(1)–Si(1)–O(1)	108(5)
O(3)–Si(1)–O(4)	114(5)
O(3)–Si(1)–O(10)	114(5)
O(4)–Si(1)–O(10)	106(5)
O(3)–Si(2)–O(2)	117(5)
O(3)–Si(2)–O(5)	110(6)
O(5)–Si(2)–O(2)	109(5)
O(9)–Si(2)–O(2)	109(5)
O(9)–Si(2)–O(3)	107(5)
O(9)–Si(2)–O(5)	104(5)
O(5)–Si(3)–O(6)	103(3)
O(5)–Si(3)–O(8)	100(3)
O(8)–Si(3)–O(6)	115(4)
O(9)–Si(3)–O(5)	111(5)
O(9)–Si(3)–O(8)	104(4)
O(9)–Si(3)–O(6)	115(4)
O(4)–Si(4)–O(7)	112(5)
O(4)–Si(4)–O(8)	100(4)
O(4)–Si(4)–O(10)	113(5)
O(8)–Si(4)–O(7)	105(3)
O(8)–Si(4)–O(10)	113(4)
O(10)–Si(4)–O(7)	114(5)

O(H)–H distances		
O(H1)–H(1)	0.85(8)	0.88(8)
O(H2)–H(2)	1.48(8)	1.21(9)
O(H3)–H(3)	0.93(11)	1.17(10)
O(H4)–H(4)	1.11(11)	1.10(11)
O(H5)–H(5)	1.15(10)	1.27(8)
O(H6)–H(6)	0.86(10)	1.52(8)
O(H7)–H(7)	1.26(10)	1.17(12)
O(H8)–H(8)	0.83(11)	1.02(11)

H(outer)–O(next layer) distances

	AHR	GDR
H(2)–O(4)	1.99(10)	2.18(10)
H(3)–O(3)	2.14(13)	1.88(12)
H(4)–O(5)	2.05(11)	2.20(10)
H(6)–O(9)	2.35(10)	1.95(9)
H(7)–O(8)	1.96(9)	2.08(10)
H(8)–O(10)	2.15(10)	1.90(11)

H(inner)–O(same layer) distances

	AHR	GDR
H(1)–O(4)apex	3.17(10)	3.30(11)
H(1)–O(7)apex	2.63(12)	2.75(11)
H(1)–O(1)apex	2.83(10)	2.80(10)
H(5)–O(6)apex	2.52(10)	2.41(10)
H(5)–O(2)apex	2.47(11)	2.52(11)
H(5)–O(9)basal	2.62(11)	2.59(11)

O(H)(outer)–H . . . O (next layer) angles

	AHR	GDR
O(H2)–H(2) . . . O(4)	142(6)	141(6)
O(H3)–H(3) . . . O(3)	148(9)	157(7)
O(H4)–H(4) . . . O(5)	146(7)	138(6)
O(H6)–H(6) . . . O(9)	134(8)	136(6)
O(H7)–H(7) . . . O(8)	153(6)	156(7)
O(H8)–H(8) . . . O(10)	141(9)	143(7)

O–H angles with a,b plane

	AHR	GDR
O(H1)–H(1)	−23(7)	−31(7)
O(H2)–H(2)	56(5)	61(7)
O(H3)–H(3)	54(11)	77(13)
O(H4)–H(4)	61(12)	55(9)
O(H5)–H(5)	10(5)	11(5)
O(H6)–H(6)	65(15)	51(4)
O(H7)–H(7)	85(17)	62(12)
O(H8)–H(8)	52(12)	53(9)

The distances and angles not involving H are from the refinement result ZRT. Those involving H are from the refinement results AHR and GDR, as indicated (see text).

culations of the H positions. These results, based on a model with the silicate tetrahedra oriented as in Newnham and Brindley (1956), are much closer to our results for the H positions than were the earlier values of Giese and Datta (1973) based on the Zvyagin (1960) model.

Hydrogen atoms

The 8 H and the 8 O(H) positions were refined from neutron data with the O, Si, and Al atoms fixed at their ZR positions. The O(H)s were refined simultaneously with the Hs because the neutron-sensed and X-ray-sensed positions of the O(H) atoms may be expected to differ a little due to the H distortion of the electron cloud sensed by X-rays around the O(H) atoms. The pattern-fitting plot for the AHR refinement is shown in Figure 5. The pattern-fitting plot for the GDR refinement, resulting from the other starting model, is essentially indistinguishable and is therefore not shown.

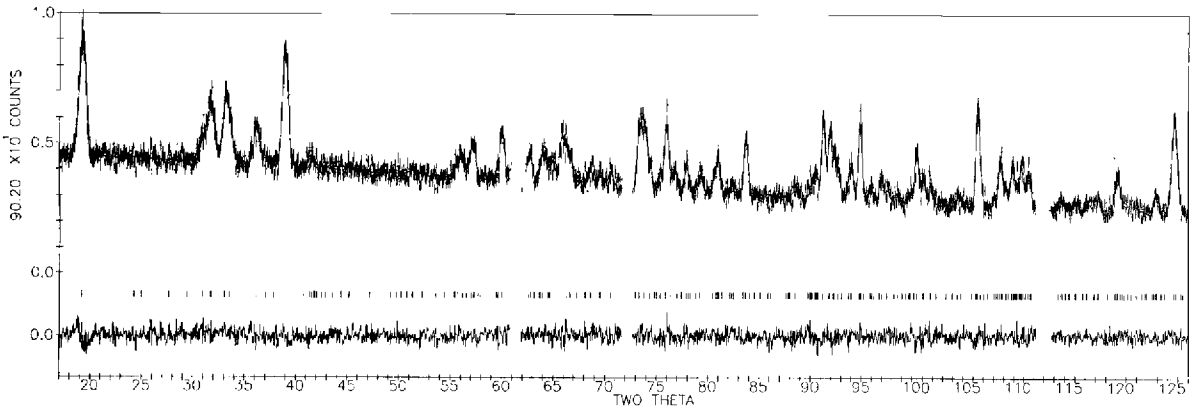

Figure 5. Pattern-fitting plot for Rietveld refinement of the H and O(H) positions with neutron data, starting with a model (AHO) based on the Adams and Hewat (1981) results for the H positions in dickite. The format is as for Figure 1.

Of the four H atoms in a half-cell, the three inner surface hydroxyl H atoms lie between the O(H) plane of one kaolinite layer and the O plane of the next one, 2.91 Å away. The fourth inner hydroxyl H is attached to an O(H) in the mixed O and O(H) plane. The H and O(H) coordinates for the two starting models and the two resulting refined models (GDR and AHR) are given in Table 3. The O–H . . . O bond angles and distances are given in Table 4 as calculated with ORFFE4 (Busing *et al.*, 1979).

As Table 4 shows, there is nothing stereochemically unusual in the O–H . . . O bond distances and angles for the H atoms which provide the hydrogen bonding that holds the layers together in kaolinite. Contrary to some previous reports (see Adams and Hewat (1981) for a discussion), all inner surface hydroxyl hydrogen atoms appear to be involved in the H bonding between layers in kaolinite; with the possible exception of H(6), all of the H–O hydrogen bond distances are within 2 σ of 2.1 Å. The H(6)–O distance is only slightly greater, and that in only one of the two measures. Further, if the AHR and GDR O–H angle results are averaged, all 6 outer O–H directions make angles of between ~53(12)° and 73(15)° with the plane of the O(H) atoms.

The most notable point of Table 4 is that the two inner hydroxyl H atoms differ decidedly in terms of how the O–H bond is directed. In the first half cell the O–H is directed into an octahedral vacancy with the hydrogen atom, H(1), being nearly equidistant from inner surface hydroxyl oxygen atoms O(H7) and O(H2) (2.05(9) and 2.36(10) Å in AHR and 2.20(8) and 2.26(11) in GDR, respectively). In the second half cell the O–H bond is directed somewhat away from the octahedral layer and toward the unoccupied center of an oxygen triangle formed by the two apical oxygens, O(6) and O(2), and the shared basal oxygen, O(9), of two adjacent SiO_4 tetrahedra. The O(H1)–H(1) distance (average of AHR and GDR) is 0.9(1) Å for the O–H pointing into the octahedral vacancy and 1.2(1) Å for the O(H5)–H(5) bond pointing toward the unoccupied center of the oxygen triangle. The angles that these two O–H directions make with the plane of the mixed O and OH sheet (parallel to a,b) are about −27(10)° and +11(7)°, respectively. The difference in the inner O–H direction is the most obvious way in which the two halves of the kaolinite cell, otherwise nearly related by C-face centering, differ.

The two starting models appear to have led to different refined positions for H(2) and H(6), which are inner surface H atoms pseudorelated by C-face centering. In both refined models, H(2) bonds to O(4) in the next layer and H(6) to O(9), but the bond distances differ. The AHR vs. GDR results for H(2) differ by 2.3 σ (combined) in x and 6.2 σ in y. For H(6) they differ by 4.8 σ in x and 8.9 σ in y. To test both for false minima and two-fold disorder of H(2) and H(6) between two positions, a half-atom (of H) was placed at each position (AHR and GDR) for H(4) and H(6) and the site occupancies were refined. The site occupancies did not change from 0.5 by more than ~10%, which is not much greater than σ. Thus, the possibility cannot be ruled out (1) the two apparent positions for H(2) and H(6) are not due to false minima, and (2) each of these atoms, H(2) and H(6), is statistically distributed equally (in two-fold disorder) between the two positions (AHR and GDR) apparently available to it.

Comparison of kaolinite and dickite

The refinement NR for dickite (Table 1 and Figure 1) was used to compare the non-H portions of the two clays because they were produced in the same way as the refinement results for kaolinite. To permit detailed comparison of the basic layer in kaolinite with that in dickite, the NR results were transformed to the BRR cell in Table 2 in the columns labeled NRT. (See Table 5 for the appropriate mapping procedure.) Except

Table 5. Labels used by various authors for the same atoms.

In kaolinite This work	Zvyagin (1960)	Newnham (1961)
Al(1)		
Al(2)	Al(2)	Al(2)
Al(3)	Al(1)	Al(1)
Al(4)		
O(1)		
O(2)		O(5)
O(3)		
O(4)	O(9)	
O(5)		O(2)
O(6)	O(4)	O(4)
O(7)	O(5)	
O(8)	O(8)	O(1)
O(9)		O(3)
O(10)	O(7)	
O(H1)	O6(H)	OH(1)
O(H2)	O2(H)	
O(H3)		
O(H4)	O3(H)	O(H3)
O(H5)		
O(H6)		O(H4)
O(H7)	O1(H)	O(H2)
OH(8)		
Si(1)		
Si(2)		Si(2)
Si(3)	Si(2)	Si(1)
Si(4)	Si(1)	

In dickite This work	Adams and Hewat (1981)	Giese and Datta (1976)
H(1)	H(1)	H(10)
H(2)	H(8)	H(8)
H(3)	H(6)	H(1)
H(4)	H(3)	H(9)
H(5)	H(5)	H(6)
H(6)	H(4)	H(2)
H(7)	H(2)	H(7)
H(8)	H(7)	H(3)

for the two inner hydroxyl oxygens, O(H1) and O(H5), the only difference $>3\ \sigma$ in the two layers are $3.6\ \sigma$ in the y and $3.9\ \sigma$ in the z of O(H5). Although some of these differences may be real, they are small and not dramatic. Even the rotations in the ·· iedral sheets are the same. This comparison of N ta with BRR data tends to confirm the near ide of the non-H parts of the basic layers of dickite and kaolinite. Clearly, the inner hydroxyl orientations constitute a major difference between dickite, in which these two H atoms are crystallographically equivalent by a C-face centering translation, and kaolinite, in which they decidedly are not.

Because dickite does not exhibit nb/3 shifting as kaolinite does, despite the fact that the non-H parts of the basic layers are essentially the same in each, the interlayer hydrogen bonding may be stronger in dickite. If so, this should be reflected in shorter H–O interlayer bond distances. From the Adams and Hewat (1981) report, the average H–O distance (for inner surface hydroxyl H atoms) is 1.90(6) Å. That for the 6 H–O distances found for kaolinite in the present work is 2.07(10) Å (averaged over both AHR and GDR results), which may be longer but is not statistically different. Likewise the average O–H . . . O angles, involving the inner surface H atoms, do not differ significantly between dickite and kaolinite (148(6)° and 144(7)°, respectively). The calculated perpendicular distance allocated per kaolinite layer is 0.0068(5) Å greater in dickite (based on the lattice parameters listed for the NRT data and BRR data in Table 1), which seems to be a statistically significant difference. It is possible, however, that systematic errors and real specimen to specimen differences may exist to produce lattice parameter differences which are this large.

CONCLUSIONS

The principal differences between dickite and kaolinite that are determinable with present experimental precision are: (1) different orientations for the two inner O–H directions in kaolinite, which alone is enough to destroy the C-face centering found in dickite, and (2) possible allocation of slightly different perpendicular distances per kaolinite layer in the two clays, perhaps reflecting the different O to O(H) interactions between layers accompanying the *c* glide plane in dickite.

ACKNOWLEDGMENTS

The authors are particularly grateful to Dr. W. D. Keller for first calling our attention to and then supplying the indispensable samples of Keokuk kaolinite and to Dr. D. E. Cox for contributing his time, skills, and limited neutron-diffractometer time. Appreciation is also expressed to Dr. W. E. Moody for his help in obtaining the specimens and for his interest and helpful discussions. This material is based in part upon work supported by the office of Surface Mining, Department of the Interior, under Grant G5105019 and continued by the Bureau of Mines under Grant G1115131.

REFERENCES

Adams, J. M. and Hewat, A. W. (1981) Hydrogen atom positions in dickite: *Clays & Clay Minerals* **29,** 316–319.

Bailey, S. W. (1963) Polymorphism of the kaolin minerals: *Amer. Mineral.* **48,** 1196–1209.

Brindley, G. W. and Nakahira, M. (1958) Further consideration of the crystal structure of kaolinite: *Min. Mag.* **31,** 781–786.

Brindley, G. W. and Porter, A. R. D. (1978) Occurrence of dickite in Jamaica; ordered and disordered varieties: *Amer. Mineral.* **63,** 554–562.

Brindley, G. W. and Robinson, K. (1946) The structure of kaolinite: *Min. Mag.* **27,** 242–253.

Busing, W. R., Martin, K. O., Levy, H. A., Brown, G. M., Johnson, C. K., and Thiessen, W. E. (1979) *ORFFE4.* Accession No. 85, World list of crystallographic computer programs, 3rd ed., *J. Appl. Cryst.* **6,** 309–346.

Giese, R. F., Jr. and Datta, P. (1973) Hydroxyl orientation in kaolinite, dickite, and nacrite: *Amer. Mineral.* **58,** 471–479.

Hayes, J. B. (1963) Kaolinite from Warsaw geodes, Keokuk region, Iowa: *Iowa Acad. Sci.* **70,** 261–272.

Keller, W. D., Pickett, E. E., and Reesman, A. L. (1966) Elevated dehydroxylation temperature of the Keokuk geode kaolinite—a possible reference mineral: *Proc. Inter. Clay Conf., 1966, Jerusalem, Israel, 1,* L. Heller and A. Weiss, eds., Israel Prog. Sci. Transl., Jerusalem, 75–85.

Newnham, R. E. (1961) A refinement of the dickite structure and some remarks on polymorphism in kaolin minerals: *Min. Mag.* **32,** 683–704.

Newnham, R. E. and Brindley, G. W. (1956) The crystal structure of dickite: *Acta Crystallogr.* **9,** 759–764.

Newnham, R. E. and Brindley, G. W. (1957) The structure of dickite: correction: *Acta Crystallogr.* **10,** p. 88.

Norton, F. H. (1973) *Elements of Ceramics:* 2nd ed., Addison-Wesley, Reading, Massachusetts, p. 17.

Rietveld, H. M. (1969) A profile refinement method for nuclear and magnetic structures: *J. Appl. Cryst.* **30,** 65–71.

Wiles, D. B. and Young, R. A. (1981) New computer program for Rietveld analysis of X-ray powder diffraction patterns: *J. Appl. Cryst.* **14,** 149–151.

Young, R. A. and Wiles, D. B. (1981) Application of the Rietveld method for structure refinement with powder diffraction data: *Adv. X-ray Anal.* **24,** 1–23.

Zvyagin, B. B. (1960) Electron diffraction determination of the structure of kaolinite: *Kristallografiya* **5,** 32–41.

(Received 18 June 1982; accepted 30 March 1983)

Резюме—На основе данных рентгеновской порошковой дифракции, обработанных по методу Ретвельда, была подробно усовершенствована кристаллическая структура каолинита ($P1$, a = 5,153(1), b = 8,941(1), c = 7,403(1) Å, α = 91,692(3)°, β = 104,860(3)°, γ = 89,822(3)°, образцы из кеокуковых жеод), а также более усовершенствована кристаллическая структура дикита (Cc, a = 5.1460(3), b = 8.9376(5), c = 14,4244(6) Å, β = 96.761(5)°). За исключением атомов водорода, слоистые структуры обоих глин являются подобными и находятся в соответствии со структурами, ранее определенными другими исследователями. Вращение в тетраэдрическом слое составляет 7(1)°. Две внутренние связи O–H в каолините ориентированы по-разному; одна направлена в сторону октаэдрической пустоты, а другая направлена немного в сторону от октаэдрического слоя и по направлению к незанятому центру кислородного треугольника, образованного из двух апикальных атомов кислорода и одного основного атома кислорода, делиного между двумя прилегающими четырехгранниками SiO_4. Все шесть атомы водорода внутренней поверхности, По-видимому, почти по-равному участвуют во водородных связях между каолинитовыми слоями в каолините. [E.G.]

Resümee—Die Kristallstruktur von Kaolinit ($P1$, a = 5,153(1), b = 8,941(1), c = 7,403(1) Å, α = 91,692(3)°, β = 104,860(3)°, γ = 89,822(3)°, Proben von Keokuk Geoden) wurden im Detail verfeinert und die von Dickit (Cc, a = 5,1460(3), b = 8,9376(5), c = 14,4244(6) Å, β = 96,761(5)° wurden noch einmal verfeinert. Bei beiden Mineralen wurde dies anhand der Röntgenpulverdaten nach der Rietveld-Methode durchgeführt. Mit Ausnahme der Wasserstoffatome sind die Lagenstrukturen in beiden Tonen sehr ähnlich und entsprechend weitgehend den Strukturen, die bereits von anderen Autoren vorgeschlagen oder bestimmt wurden. Die Rotation in den Tetraederschichten beträgt 7(1)°. Die beiden inneren Hydroxyl O–H Bindungen im Kaolinit sind unterschiedlich orientiert; die eine zeigt in eine oktaedrische Lücke und die andere etwas von der Oktaederschicht weg und in Richtung des unbesetzten Zentrums eines Sauerstoffdreiecks, das durch zwei apicale Sauerstoffe und dem gemeinsamen Sauerstoff von zwei benachbarten SiO_4-Tetraedern gebildet wird. Alle sechs inneren Oberflächen-Wasserstoffatome scheinen nahezu zu gleichen Teilen an der Wasserstoffbindung zwischen den Kaolinitlagen im Kaolinit beteiligt zu sein. [U.W.]

Résumé—La structure cristalline de la kaolinite ($P1$, a = 5,153(1), b = 8,941(1), c = 7,403(1) Å, α = 91,692(3)°, β = 104,860(3)°, γ = 89,822(3)°, spécimens de géodes de Keokuk) a été raffinée en détail, et celle de la dickite (Cc, a = 5.1460(3), b = 8,9376(5), c = 14,4244(6) Å, β = 96,761(5)°) a été re-raffinée, toutes deux à partir de données de diffraction avec la méthode de Rietveld. A part les atomes d'hydrogène, les structures de couches dans les deux argiles sont très semblables et sont proches de ce que d'autres avaient précedemment inféré ou déterminé. La rotation dans le feuillet tétraèdral est 7(1)°. Les deux liens intérieurs hydroxyls O–H dans la kaolinite sont orientés différemment; l'un se dirige vers un site octaèdral vacant, et l'autre quelque peu dans une direction opposée à la feuille octaèdrale et vers le centre inoccupé d'un triangle oxygène formé par les deux oxygènes apiquaux et l'oxygène basal partagé par deux tetràedres SiO_4 adjacents. Les six atomes d'hydrogène de la surface intérieure semblent etre presque également impliqués dans les liens d'hydrogène entre les couches de kaolinite dans la kaolinite. [D.J.]